THE JOURNAL OF PHYSICAL CHEMISTRY B

Article

pubs.acs.org/JPCB

Time-Resolved Single Molecule Fluorescence Spectroscopy of an α-Chymotrypsin Catalyzed Reaction

Tatyana G. Terentyeva,[†] Johan Hofkens,[†] Tamiki Komatsuzaki,[‡] Kerstin Blank,*[,§] and Chun-Biu Li*[,‡]

[†]Photochemistry & Spectroscopy, Department of Chemistry, Katholieke Universiteit Leuven, Leuven, Belgium

[‡]Molecule & Life Nonlinear Sciences, Research Institute for Electronic Science (RIES), Hokkaido University, Sapporo, Japan

[§]Institute for Molecules and Materials, Radboud University Nijmegen, Nijmegen, The Netherlands

Supporting Information

ABSTRACT: Single molecule fluorescence spectroscopy offers great potential for studying enzyme kinetics. A number of fluorescence reporter systems allow for monitoring the sequence of individual reaction events with a confocal microscope. When using a time-correlated single photon counting (TCSPC) detection scheme, additional information about the fluorescence lifetimes of the fluorophores can be obtained. We have applied a TCSPC detection scheme for studying the kinetics of α-chymotrypsin hydrolyzing a double-substituted rhodamine 110-based fluorogenic substrate in a two-step reaction. On the basis of the lifetime information, it was possible to discriminate the intermediate and the final product. At the high substrate concentration used, only the formation of the intermediate was observed. No rebinding of the intermediate followed by rhodamine 110 formation occurred at these high concentrations. We have further found no alterations in the fluorescence lifetime of this intermediate that would indicate changes in the local environment of the fluorophore originating from strong interactions with the enzyme. Our results clearly show the power of using lifetime-resolved measurements for investigating enzymatic reactions at the single molecule level.

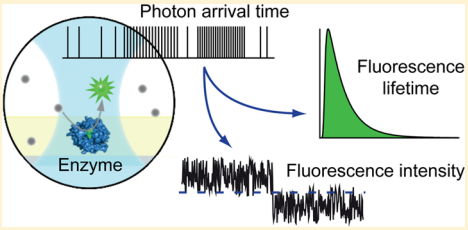

INTRODUCTION

Since their discovery, the superior catalytic activity and selectivity of enzymes has been a subject of intensive research with the goal of understanding the structural origin of these unique properties. Enzymes are protein molecules consisting of a linear chain of different amino acids that is folded into a complex three-dimensional structure. This structure, which is not static and constantly exposed to thermal fluctuations, determines the enzymatic activity. It is now well recognized that dynamic changes between different enzyme conformations are crucial for the function of many enzymes.[1−3]

Over the last 20 years, the developments in single molecule fluorescence spectroscopy have provided methods to observe dynamic processes at the level of individual molecules, including enzymes.[4,5] To follow these molecular processes in real time and to link them to the enzyme's biological function, a number of fluorescence reporter systems based on different detection principles have been developed. For example, enzyme conformational changes, eventually linked to the catalytic activity, have been detected on the basis of fluorescence resonance energy transfer (FRET)[6−9] or electron transfer (ET).[10,11] The incorporation of fluorescent probes into natural substrates (e.g., DNA strands) has been used to study the enzymatic cleavage of these substrates, e.g., in DNA sequencing reactions.[12−15] Another approach is the tracking of fluorescently labeled enzymes as they move on their natural substrates.[16,17] The most general and direct approach to follow the catalytic reaction is the use of fluorogenic substrates or cofactors, as their fluorescence is altered as a result of the enzymatic reaction.[18−22]

Using these reporter systems, the molecular process can be recorded down to the level of individual reaction events using a confocal microscope setup. The use of avalanche photodiodes (APDs) as single photon counting detectors provides the sensitivity and time resolution needed to detect single fluorophores produced in the enzymatic reaction or reporting on conformational changes. Using a pulsed excitation laser, time-resolved detection with an APD does not only record the number of photons emitted by the fluorescence reporter system, it also yields information about the fluorescence lifetime of the fluorophore. This time-correlated single photon counting (TCSPC) approach provides the absolute photon arrival time with respect to the start of the measurement (macrotime) together with the arrival time relative to the last laser pulse (microtime). In addition to the lifetimes, information about fluorescence polarization can potentially be obtained in a TCSPC detection scheme by exciting the sample with polarized light and by separating the emitted photons into two orthogonal polarization directions, collected with two detectors.[23−25]

Most frequently, only the macrotime information is used in subsequent data analysis procedures to calculate an intensity (photons/time) time trace. This intensity time trace is

Received: October 28, 2012
Revised: January 8, 2013
Published: January 11, 2013

Scheme 1. Two-Step Hydrolysis of (Succinyl-AlaAlaProPhe)$_2$-Rh110 by α-Chymotrypsin[a]

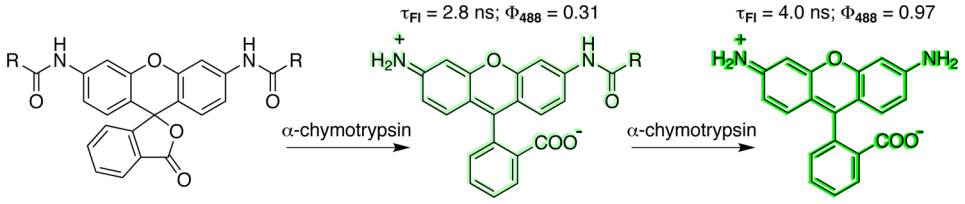

[a]Fluorescence lifetimes τ_{Fl} and quantum yields Φ_{488} of the intermediate and the Rh110 product are shown.

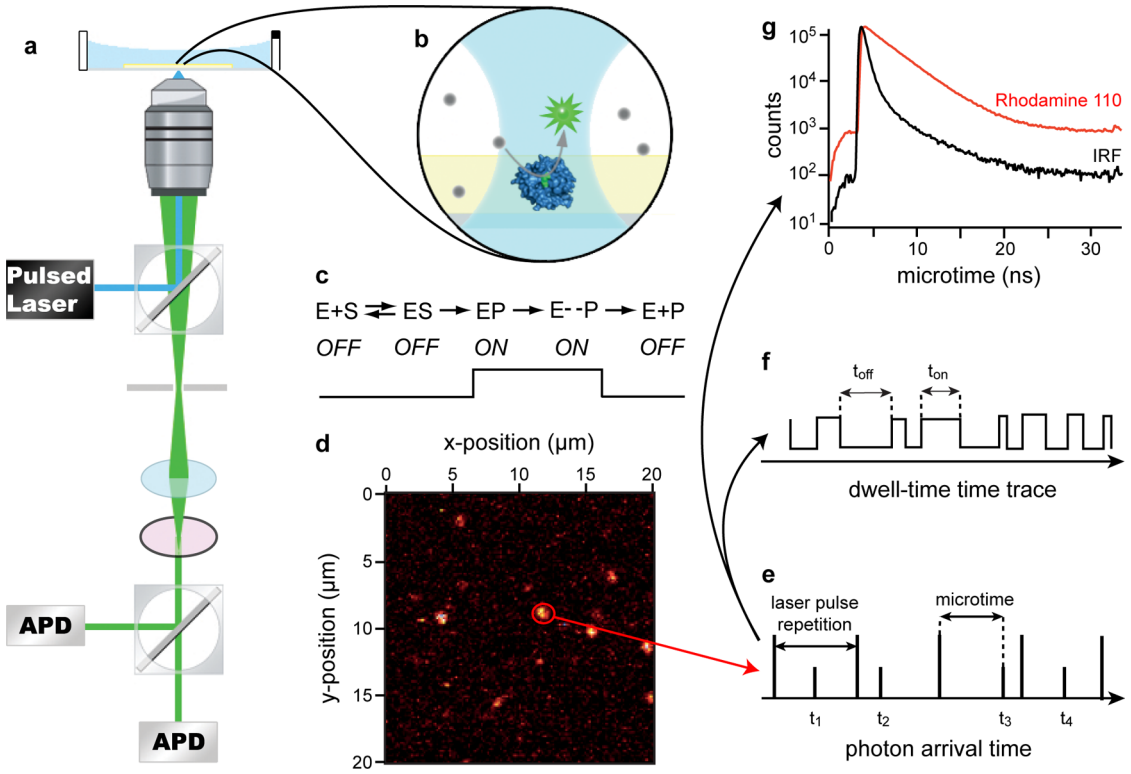

Figure 1. Experimental setup. (a) Inverted confocal fluorescence microscope with pulsed laser excitation, a polarized beam splitter and two APD detectors. This setup is used to follow the formation of fluorescent molecules by an immobilized enzyme (b) according to the on/off state kinetic scheme (c). After positioning the laser focus on the spot of the enzyme (d), macro- and micro-photon arrival times are recorded with TCSPC (e). From the macrotime t_n, the dwell time trace is obtained (f). The microtime distribution yields the fluorescence lifetime (g).

subsequently used to determine the different intensity levels and their corresponding dwell times. Due to the intrinsic noise of the measurement, the assignment of intensity levels is difficult, however. The assignment is especially challenging if the dwell times of the different intensity levels are very short and/or if they contain only a small number of photons (<200).[26] For FRET and ET measurements, it has been shown that the accuracy of this assignment can be improved by complementing the intensity−time traces with the microtime information. When utilizing the microtimes to determine the fluorescence lifetime, different molecular states can be identified more easily even if the intensity levels overlap and the population(s) of interest can be selected for further analysis.[24,25]

Microtime information has not yet been used to improve the assignment of the different intensity levels when using fluorogenic substrates. In the on-state, i.e., when a fluorescent enzymatic product is present in the detection volume, the photons clearly originate from the fluorescent product. In the off-state, however, the photons might originate from different sources such as Raman scattering and impurities. Fluorescent products can further have different molecular states (e.g., enzyme-bound and unbound states), which might be observed on the basis of differences in their fluorescence lifetime.

Under specific experimental conditions, the fluorescence lifetime is characteristic for a given fluorophore and can be used to identify a fluorescent dye in a mixture of several different dye molecules.[27,28] The fluorescence lifetime is further a sensitive marker for environmental influences, such as changes in the refractive index, the presence of quenchers, or changes in the pH value. The close proximity of a protein or another macromolecule can, therefore, alter the lifetime of a fluorophore.[10,29,30] Consequently, the lifetime of an enzyme-bound fluorescent product (on-state) might be different from freely diffusing product molecules and the other processes contributing to the off-state. On the basis of this, the fluorescence lifetimes might be a useful additional parameter to assist the correct assignment of different states of the enzymatic reaction.

dx.doi.org/10.1021/jp310663v | J. Phys. Chem. B 2013, 117, 1252−1260

In addition to the potential of improving the on−off assignment, the analysis of fluorescence lifetimes might further resolve important substeps of the enzymatic hydrolysis of double-substituted fluorogenic substrates based on rhodamine 110 (Rh110) or fluorescein.[31−34] Both Rh110- and fluorescein-based substrates contain two enzyme cleavable bonds. For Rh110-based protease substrates, we have recently shown that the first cleavage product (in the following called intermediate) is also fluorescent but has a different brightness and fluorescence lifetime as the second cleavage product Rh110 (Scheme 1).[35] Consequently, it might be possible to discriminate these two different fluorescent species that are produced by the enzymatic reaction.

To investigate which additional information can be obtained from lifetime detection applied to the enzymatic cleavage of a double-substituted Rh110-based substrate, we have measured the time series of individual turnovers of the enzyme α-chymotrypsin hydrolyzing the substrate (succinyl-AlaAlaPro-Phe)$_2$-Rh110. Using a TCSPC approach, we have recorded both the macrotimes and the microtimes. In the data analysis, we have focused on the following three questions: (i) is the multiparameter approach useful to reach an improved assignment of the on- and the off-states, (ii) do we observe differences in the lifetimes between the on- and off-states that point toward any changes in the local environment of the fluorophore, and (iii) is it possible to observe the two different enzyme produced fluorescent species based on their different intensities and fluorescence lifetimes? The latter would add to our understanding of the kinetics of this two-step cleavage reaction. It is currently not known if the intermediate is released and accumulates in solution or if the intermediate undergoes some rotational motion and is immediately cleaved by the enzyme to yield Rh110 (known as the tunneling or channeling effect).[33,34]

EXPERIMENTAL METHODS

Sample Preparation. Fluorescently labeled α-chymotrypsin molecules were immobilized by entrapment in an agarose matrix on a glass coverslip. Prior to immobilization, the glass coverslips were cleaned by sonication in acetone, then in ultrapure water, followed by baking them in a clean oven at 450 °C for 12 h. After carefully rinsing with ultrapure water, they were again baked in the oven. Finally, they were subjected to UV/ozone treatment to bleach any remaining fluorescent impurities. The enzyme α-chymotrypsin (from bovine pancreas, Fluka) was labeled with 5-(and-6)-FAM (5-(and-6)-carboxyfluorescein succinimidyl ester, mixed isomers; Invitrogen) to be able to locate individual enzyme molecules on the surface. Labeled enzymes (degree of labeling: two dyes/enzyme) were diluted to a final concentration of 0.05 nM enzyme in a solution of 1% (w/v) agarose in ultrapure water at 30 °C. This solution was spin-coated onto the cleaned glass coverslips. The coverslip was immediately placed into a sample holder, and 1 mL of PBS (0.01 M phosphate pH 7.4, 138 mM NaCl, 2.7 mM KCl) was added on top of the coverslip. The sample was kept at room temperature until the measurement.

Optical Setup. Time-resolved fluorescence detection was performed with an optical setup that is described elsewhere.[36] Briefly, turnovers of individual α-chymotrypsin molecules were detected with a stage scanning inverted confocal fluorescence microscope (Olympus IX70) equipped for time-correlated single photon counting (Figure 1). The sample was illuminated with 488 nm pulsed laser light (8.13 MHz repetition rate) from a mode-locked Ti:sapphire laser (Tsunami, Spectra Physics). The excitation light was filtered with a 490 ± 10 nm excitation filter (Linos) and circularly polarized with a Berek compensator. Using neutral density filters, the excitation power was adjusted to a value between 1 and 10 μW before entering the microscope objective. The excitation light was focused via an oil immersion objective (Zeiss, 1.3 N.A., 100×). The emitted fluorescence was collected by the same objective. After passing a dichroic beam splitter, the emitted light was focused through a 100 μm pinhole and filtered by a 500 nm long-pass emission filter (Linos) as well as a band-pass 520/40 nm filter (Linos). The emission path further contains a polarizing beam splitter cube (Newport) separating the emitted photons into two orthogonally polarized directions before counting them with two separate avalanche photodiodes (SPCM-AQR-15, Perkin Elmer). The information from each APD (time jitter ∼400 ps) was collected using a time-correlated single photon counting (TCSPC) computer card (Becker&Hickl GmbH, SPC 630).

Single Enzyme Measurements. The sample holder was placed onto the confocal microscope. To locate individual fluorescently labeled enzymes on the coverslip, the surface (20 μm × 20 μm) was scanned to obtain an image of the fluorescence intensity at each position of the sample, utilizing the piezoelectric translation stage (Physik Instrumente) of the confocal microscope. The enzyme molecules were visible as bright spots in the scanned images. After placing the confocal spot at the position of an enzyme, the catalytic reaction was started by adding 1 mL of a 60 μM solution of the fluorogenic substrate (succinyl-AlaAlaProPhe)$_2$-Rh110 in PBS (30 μM final concentration). The synthesis and purification of the substrate is described elsewhere.[21] After bleaching the fluorescent labels coupled to the enzyme for several seconds, the time series of enzymatic turnovers was monitored as a series of photon arrival times for 1600 s. The ensemble kinetic parameters of the α-chymotrypsin catalyzed hydrolysis of (succinyl-AlaAlaProPhe)$_2$-Rh110 are k_{cat} = 0.43 s^{-1} and K_M = 8 μM. It is essential to note that these are apparent kinetic parameters of the double cleavage reaction where a mixture of the low fluorescent, monohydrolyzed intermediate and the final product Rh110 is measured. The kinetic parameters describing the two hydrolysis steps separately cannot be resolved with an ensemble measurement.[35]

Determination of the "On" and "Off" States. Change point analysis was applied to the photon arrival time trace (macrotimes) to determine the intensity levels of the on- and off-states of the catalytic cycle. Details of this method have been described by Watkins and Yang[37] and by Terentyeva et al.[26] In brief, by treating the detection of a change point as a statistical hypothesis test, the probability that a photon in the time trace is an intensity change point is calculated and compared to the probability that the photon considered is not a change point. A change point is declared to exist if a given confidence level is reached. The location of the change point is assigned to the photon with the largest likelihood of being a change point. The above procedure is then repeated with binary segmentation in order to detect multiple change points in the photon trace. The segmentation procedure stops when no new change points can be found with the given confidence level anymore. Because of undesired intensity fluctuations originating from various types of noise in the experiment, the change point detection is followed by a clustering procedure to assign the detected change point intervals to the on/off-states. This is done by subjecting all change point intervals to a second change point

detection step to identify the boundary between the "on" and "off" intensity levels. Finally, consecutive on/off change point intervals are combined, yielding the "on" and "off" dwell time sequence. After clustering, also the signal-to-noise (S:N) ratio was determined as the ratio of the average intensity of the on- and off-states. The average intensity was calculated from the total number of photons in all on/off-states divided by the duration of all on/off-states, respectively. Only time traces that showed a S:N ratio close to or higher than 2.5:1 have been considered for further analysis.

Data Analysis. The results of the change point analysis and the subsequent clustering procedure provide the sequence of on- and off-states from which the photophysical properties (intensity and lifetime) can be extracted statistically. These properties can be determined for the cumulated on-states or off-states by collecting all photons belonging to all on-states or all off-states, respectively. Alternatively, the determination of the photophysical properties can be done for all individual dwell times of both the on- and off-states.

Fluorescence Intensity. The intensity of a given on- (or off-) state was estimated using maximum likelihood methods.[38] In particular, for a given state with the number of photons N and the duration T, the maximum likelihood estimation (MLE) of the intensity I_{ML} is given by the value that maximizes the log-likelihood function; i.e., $\log P_1(N|I, T)$ is maximized at $I = I_{ML}$ with the likelihood function given by the Poisson distribution: $P_1(N|I, T) = (IT)^N e^{-IT}/N!$. A simple calculation results in $I_{ML} = N/T$. On the other hand, the error in the MLE of the intensity can be found by the use of the Cramér−Rao inequality.[39,40] The Cramér−Rao inequality states that the variance $\mathrm{var}(I_{ML})$ in the MLE of an unknown parameter (the intensity in this case) is more than or equal to the inverse of the Fisher information $J(I_{ML})$:

$$\mathrm{var}(I_{ML}) \geq \frac{1}{J(I_{ML})}$$

where the Fisher information is defined by the expectation value of the second derivative of the log-likelihood function:

$$J(I) = -E_{P_1(N|I,T)}\left[\frac{\partial^2 \log P_1(N|I, T)}{\partial I^2}\right] = -\sum_{N=0}^{\infty} P_1(N|I, T)\frac{\partial^2 \log P_1(N|I, T)}{\partial I^2}$$

Intuitively, the Fisher information may be thought of as a measure of the broadness of the log-likelihood function. A sharp log-likelihood function gives rise to a larger value of $J(I_{ML})$ and therefore a smaller variance $\mathrm{var}(I_{ML})$ in the MLE of the intensity, as suggested by the Cramér−Rao inequality. We take the inverse of the Fisher information as the error in the MLE (i.e., $\Delta I = (1/J(I_{ML}))^{1/2}$), and a straightforward calculation of the Fisher information leads to $\Delta I = (N)^{1/2}/T$.

Fluorescence Lifetimes. Microtime histograms are commonly used for the determination of the fluorescence lifetime. As the cumulated on- (or off-) states contain a large number of photons (>1000), the corresponding microtime histograms are well sampled and the histograms can be fitted directly using commonly applied time-resolved fluorescence analysis software based on least-squares fitting.[41] For the individual on- or off-states, however, the number of photons is small. Instead of fitting a poorly sampled histogram, the fluorescence lifetimes of the individual states were again determined using maximum likelihood estimation on a photon-by-photon basis.

The maximum likelihood estimation of the fluorescence lifetime τ_{ML} of an individual on- (or off-) state was performed in a similar way as for the intensity. Now the log-likelihood function $\log P_2(\{\tau_i\}|\tau)$ was maximized with respect to the lifetime τ. Here $\{\tau_i\} = \{\tau_1, \tau_2, ..., \tau_n\}$ denotes the set of microtimes of the N photons in a given on- (or off-) state. By assuming that the microtimes are independent and identically distributed, the likelihood function to be maximized reads

$$P_2(\{\tau_i\}|\tau) = \prod_{i=1}^{N} (a e^{-\tau_i/\tau} + b)$$

where a is the normalization constant and b is the probability corresponding to the counts of background photons. The error of the MLE of the lifetime $\Delta\tau$ can be estimated similarly as in the case of intensity estimation by using the Fisher information

$$J(\tau) = -E_{P_2(\{\tau_i\}|\tau)}\left[\frac{\partial^2 \log P_2(\{\tau_i\}|\tau)}{\partial \tau^2}\right] = -\int_0^{\infty} d\tau_1 d\tau_2 ... d\tau_N P_2(\{\tau_i\}|\tau)\frac{\partial^2 \log P_2(\{\tau_i\}|\tau)}{\partial \tau^2}$$

and the Cramér−Rao inequality. Different from the case of the intensity, where an analytical solution can be obtained, the maximization of the likelihood function and the evaluation of the Fisher information in the microtime case were performed numerically.

To construct the cumulated microtime histograms, the microtimes of all photons belonging to all assigned on- (or off-) states were extracted and accumulated into one histogram for the on-states and one histogram for the off-states, respectively. The obtained fluorescence decay histograms were then used for the determination of the fluorescence lifetimes. The analysis was performed using time-resolved fluorescence analysis (TRFA) software (www.sstcenter.com) that takes pulse deconvolution into account. A nonlinear least-squares fitting of the lifetimes was performed by minimizing the reduced chi-square (χ^2) based on the Marquardt algorithm. The algorithm uses a reweighted iterative reconvolution method of the instrumental response function (IRF) with a monoexponential and double-exponential model.[42] The quality of the fit was judged on the basis of the values of the chi-square and a visual inspection of the fit, the residuals, and the autocorrelation function.[43] The IRF was measured with a droplet of an aqueous solution of erythrosine on the glass coverslip. Since its lifetime is very short (87 ps), this method gives a good representation of the IRF.[41]

Construction of 2D Correlograms. In order to provide an intuitive visualization of the possible correlations between two observables (e.g., intensity and lifetime), 2D correlograms have been constructed in terms of the summation of 2D Gaussian distributions for all the on- (or off-) states as

$$d(x, y) = \sum_{i=1}^{N_{event}} w_i G(x|x_{ML}, \Delta x^2) G(y|y_{ML}, \Delta y^2)$$

where N_{event} is the number of on- (or off-) events, x_{ML}, y_{ML}, Δx, and Δy are the MLE of the observable x, y and their uncertainties, respectively. $G(x|x_{ML}, \Delta x^2)$ denotes the Gaussian distribution with mean x_{ML} and variance Δx^2. The weight $w_i = T_i/T_{total}$ of an on- (or off-) state is determined by the ratio of its

dx.doi.org/10.1021/jp310663v | J. Phys. Chem. B 2013, 117, 1252−1260

duration T_i to the total time length of all on- (or off-) states $T_{total} = \sum_{i=1}^{N_{event}} T_i$.

RESULTS AND DISCUSSION

Determination of Enzymatic Turnovers. In general, when measuring the enzymatic hydrolysis of a fluorogenic substrate with single turnover resolution, every enzymatic turnover is considered to produce a fluorescent molecule that results in a high fluorescence intensity period, denoted here as the on-state. These on-states are separated by low fluorescence intensity periods (off-states) when no fluorescent product molecules are present in the detection volume (Figure 1c). α-Chymotrypsin hydrolyzes the fluorogenic substrate (succinyl-AlaAlaProPhe)$_2$-Rh110 in a two-step reaction (Scheme 1). In this two-step reaction, the intermediate succinyl-AlaAlaProPhe-Rh110 is produced first. It is then further hydrolyzed by the enzyme to yield the fluorescent dye Rh110. The intermediate is also fluorescent. Whereas its emission maximum is approximately at the same wavelength as the emission maximum of Rh110, it differs in its quantum yield and the fluorescence lifetime. The intermediate has a quantum yield of 0.31 and a lifetime of 2.8 ns, while Rh110 has a quantum yield of 0.97 and a lifetime of 4 ns.[35] Every catalytic cycle of the enzyme yielding either the intermediate or the final product Rh110, therefore, produces a fluorescent molecule. In our single molecule detection scheme, two scenarios are possible based on the relatively low quantum yield of the intermediate: (i) The fluorescence intensity of the intermediate is too low to be determined as a clear on-state. Being "counted" as an off-state, it contributes to the background fluorescence. Only the production of the final product Rh110 will be detected as an on-state of the reaction, and a high number of enzymatic turnovers will be "lost" in our detection scheme. (ii) The fluorescence intensity of the intermediate is sufficiently high to be detected as an on-state. In this case, every enzymatic reaction event can be observed. Since the brightness and the fluorescence lifetime of both the intermediate and the Rh110 are different, it is expected that two intensity populations characterized by different lifetimes are observed in the on-state.

In order to obtain a large number of enzymatic turnovers (>1000; on-states), required for a statistical analysis, α-chymotrypsin was immobilized in an agarose matrix. This immobilization method confines enzyme molecules such that no translational diffusion of the enzyme is taking place, while at the same time the rotational diffusion is not affected (see the Supporting Information). Using the TCSPC confocal microscope setup, we were able to follow the time series of events for at least 10 individual immobilized α-chymotrypsin molecules for hundreds of seconds. All photon arrival time traces were subjected to change point analysis to determine the dwell time trajectories of the enzymatic reaction as well as the S:N ratios. Only time traces that showed S:N ratios of approximately 2.5:1 or higher were used for further analysis (three enzymes).[26] The time trace of the enzyme discussed in the following had a S:N ratio of 2.4 and a "noise" intensity of approximately 10 000 photons/s (see the Supporting Information for a representative section of the binned time trace as well as the results from two other enzymes).

The dwell time histograms of the on- and off-states are shown in Figure 2. These histograms are similar to earlier published results.[26] The total number of on-states was 67 500 with $\langle t_{off} \rangle$ = 0.023 s and $\langle t_{on} \rangle$ = 0.001 s. Dividing the total number of on-states by the total measurement time of 1600 s, a turnover frequency of 42 turnovers/s was obtained (12 and 13 s^{-1} for two additional enzymes in the Supporting Information). This rate is almost 100 times higher than the apparent k_{cat} of 0.43 s^{-1} determined in the ensemble measurement where a mixture of the low fluorescent intermediate and Rh110 is detected simultaneously. In the ensemble measurement, the enzymatic rate is underestimated, as mostly the low-fluorescent intermediate is produced under initial rate conditions. The single molecule turnover frequency needs to be compared to the ensemble reaction rate of a "clean" one-step cleavage reaction that we have determined previously.[35] The kinetic constants of the corresponding monosubstituted morpholine-carbonyl-Rh110 derivative are K_M = 68 μM and k_{cat} = 11 s^{-1}. As we have used substrate concentrations above the apparent K_M value in our single molecule experiment, it can be assumed that the measurement was performed under reaction-controlled conditions enabling a comparison of the enzymatic rates. The high turnover frequency, that matches the corresponding ensemble rate within a factor of 3.5, consequently gives a first indication that it is actually possible to determine every enzymatic turnover including both the production of Rh110 and the low-fluorescent intermediate.

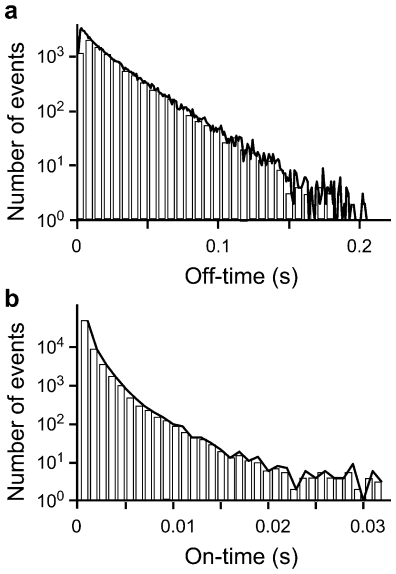

Figure 2. Dwell time histograms for the off- (a) and on-states (b) of a representative enzyme (bin width 0.001 s). Dwell times of the enzyme turnovers have been obtained with change point analysis of a photon arrival trace of 1600 s. Average dwell times: $\langle t_{off} \rangle$ = 0.023 s, $\langle t_{on} \rangle$ = 0.001 s.

It should be noted here that the dwell time histogram of the on-states shows deviations from single-exponential kinetics (Figure 2b). This is no proof, however, that different molecular species are produced in the enzymatic reaction. We have shown previously using simulated data that deviations from single-exponential kinetics in the on-histograms can also originate from a kinetic scheme where the fluorescent on-state consists of more than one state in the kinetic scheme such as the enzymatic reaction followed by product diffusion.[26] Consequently, it is not possible to deduce from the on-histogram that both the intermediate and the final product are produced in our experiment. In order to clarify the underlying kinetic scheme, time series analysis would be required to extract the underlying state network from the observed on/off time series.[44−47]

dx.doi.org/10.1021/jp310663v | J. Phys. Chem. B 2013, 117, 1252−1260

Lifetime Analysis. To facilitate a more detailed analysis, that reveals possible correlations between the intensities and the lifetimes of the off- and on-states, these two parameters were determined with MLE for each state. Figure 3 shows the 2D correlogram of the lifetimes vs the intensities for both the on- and off-states.

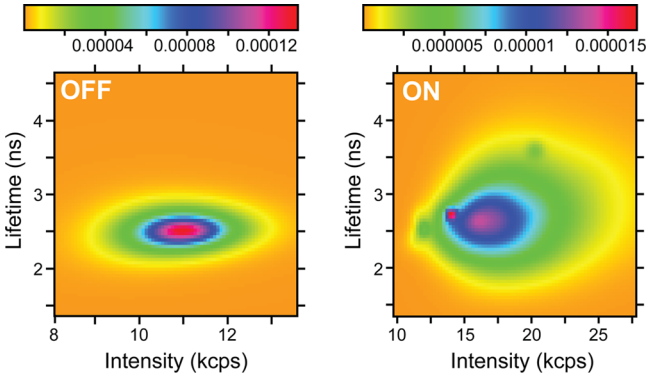

Figure 3. 2D correlograms of fluorescence lifetimes vs intensity for the off- and on-states of the enzyme displayed in Figure 2. These correlograms have been constructed in terms of the summation of 2D Gaussian distributions of the MLE for all the off-states and the on-states. The color scale labels the numerical value of the distributions in arbitrary units.

For the enzyme molecule shown in Figure 2, the correlogram for the off-states shows only one clearly defined population that has a maximum at an intensity of 11 000 photons/s and a lifetime of 2.6 ns. Also, the on-states show one main population with a maximum at 17 000 photons/s and 2.7 ns. For the on-states, however, both the intensities and the lifetimes show a much broader distribution. No correlations between intensities and lifetimes are observed. Similar results were obtained for the two other enzymes measured (see the Supporting Information; the Supporting Information also contains a discussion of the possible origin of the additional populations in the on-correlogram).

The lifetimes determined from the 2D correlograms correspond to the lifetime of the succinyl-AlaAlaProPhe-Rh110 intermediate of the reaction (2.8 ns). The characteristic lifetime of Rh110 itself (4 ns) is not present in the correlograms. The broadening of the on-population in the 2D correlograms might be caused by some environmental influences on the dye or, most likely, by the statistical error originating from the small number of photons per state. The uncertainties in the MLE fitting procedure scale with $1/N^{1/2}$, with N being the number of photons in a given on- or off-state. The ratio of the average number of photons in an off-state (250) to the average number of photons in an on-state (25) is roughly 10. Consequently, the uncertainties in determining the lifetimes of the on-states are 3 times larger than the uncertainties in the off-state lifetimes. The broadening of the

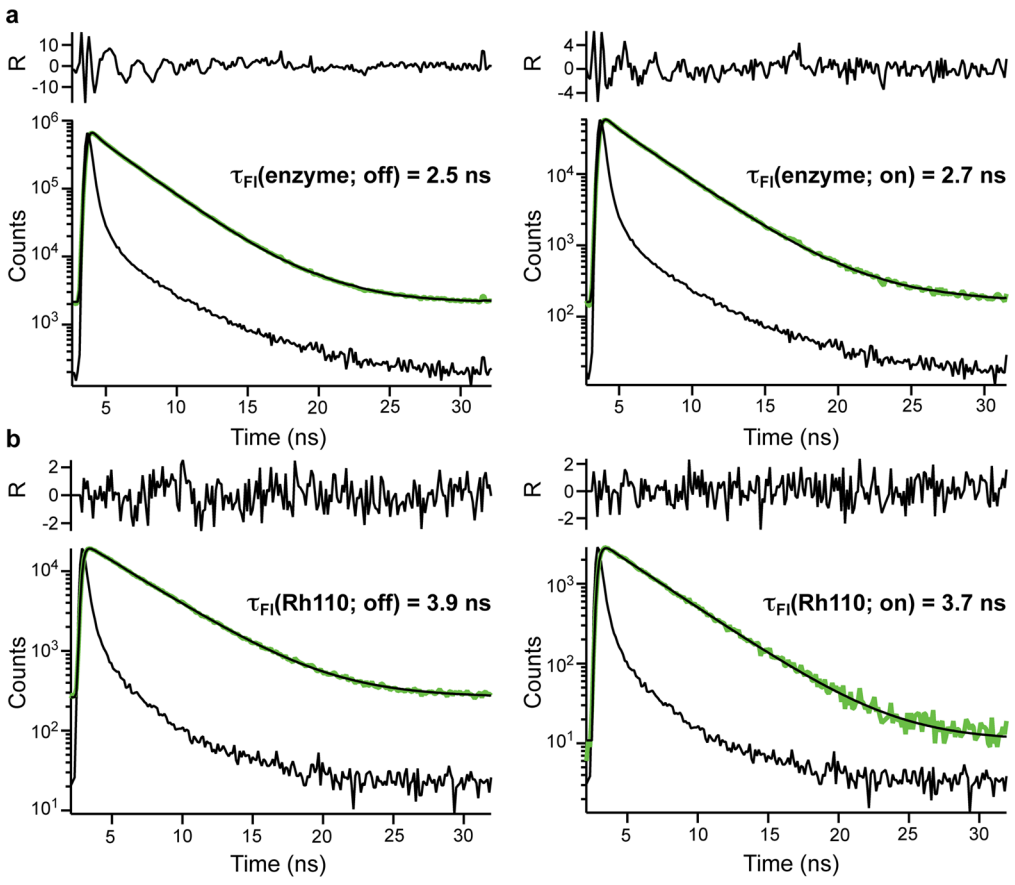

Figure 4. Fluorescence decay histograms for the cumulated on- and off-states. (a) Enzyme turnover data; (b) control experiment with Rh110. All microtimes of the photons assigned to the off-states (left column) and to the on-states (right column) were extracted and used to build their corresponding decay histograms (green lines). These decays were fitted using a deconvolution of the IRF signal (black peak). The fits are shown in black on top of the experimental data (green lines). The fit residuals are depicted above the corresponding graphs.

dx.doi.org/10.1021/jp310663v | J. Phys. Chem. B 2013, 117, 1252−1260

on-population in the 2D correlogram lies well within this factor of 3, leading to the conclusion that the on- and off-states cannot be discriminated on the basis of their lifetimes.

It might be questioned why we are talking about fluorescence lifetimes for the off-states (background photons). The fact that an exponential lifetime decay is observed for the off-states can be attributed to fluorescent intermediate and/or product molecules that are present in the sample at any time during the measurement. If a fluorescent molecule diffuses through the detection volume quickly or passes by at the edge of the confocal volume, a small number of photons will be detected. These photons are not sufficient to be detected as an on-state. However, the microtimes of all these photons are continuously contributing to the measurement. Interestingly, for both the on-states and the off-states, only one population with the lifetime of the intermediate is observed. This result clearly suggests that the intermediate is the main source of photons in the off-state and that no other processes contribute to the background significantly.

The absence of the lifetime population of 4 ns was unexpected. To confirm that the observation of this population is not limited by the small number of photons in the MLE estimation, we have analyzed the lifetime distributions in more detail. All microtimes detected for the assigned off-states and the on-states have been extracted and used to build cumulated fluorescence decay histograms (Figure 4). These histograms were fitted with a biexponential decay. The lifetimes obtained from these fits are 2.5 ns (90%) and 0.3 ns for the off-states and 2.7 ns (91%) and 0.3 ns for the on-states, confirming that the main species detected in both states is the intermediate. The 0.3 ns component is most probably originating from scatter that is not fully filtered out. Note that this decay time is shorter than the detection limit of the APD used (~400 ps).

To further confirm the accuracy of this result and to clearly eliminate the possibility that it originates from errors in the detection or the data analysis, we have measured Rh110 under identical experimental conditions as a control experiment. A Rh110 solution (1 nM) was added to an agarose gel containing fluorescently labeled and immobilized enzymes. After focusing the laser spot on a position in the sample where a labeled enzyme was located and after bleaching the label, fluorescent Rh110 molecules diffusing through the detection volume were measured. The analysis of this Rh110 control data was performed exactly in the same way as for the catalysis data and revealed an average on-time of approximately 0.5 ms. The fluorescence lifetimes determined from the MLE are again plotted in a lifetime vs intensity 2D correlogram (Figure 5). The lifetime of the individual on- and off-states for the freely diffusing Rh110 is 3.5 ns for both the on- and off-states. From fitting the fluorescence decay histograms of the cumulated photons of all on/off-states, fluorescence lifetimes of 3.9 ns (95%) and 0.3 ns were obtained for the off-states and 3.7 ns was obtained for the on-states (Figure 4). These lifetimes correspond well to the known lifetime of Rh110 (4 ns) measured freely diffusing in aqueous solution. The small difference between the lifetime of the dye in solution and the dye diffusing in the agarose gel might be due to inhomogeneous environmental influences where lifetime differences are induced by various effects such as the refractive index, interactions with the enzyme or the agarose matrix, and the local polarity and polarizability.[41,48] These effects might also be responsible for the small additional population in the on-correlogram and are discussed in more detail in the Supporting Information.

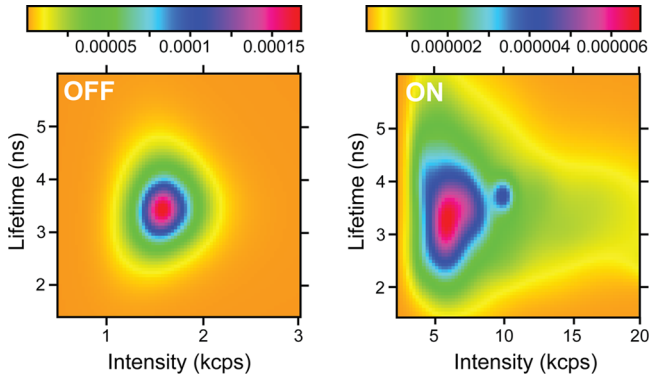

Figure 5. 2D correlograms of fluorescence lifetimes vs intensity for the off- and on-states for the Rh110 control experiment. These correlograms have been constructed in terms of the summation of 2D Gaussian distributions of the MLE for all the off-states and the on-states. The color scale labels the numerical value of the distributions in arbitrary units.

It is, therefore, possible to discriminate lifetime differences with our experimental approach. This result confirms that the main species present is the intermediate of the enzymatic reaction. As the intermediate shows the same lifetime in both the on-state and the off-state, possible interactions between the enzyme and the intermediate appear to be unlikely. From this result and the average on-time in the Rh110 control experiment, it can be tentatively concluded that the duration of an enzymatic on-time is mostly determined by the diffusion of the reaction product in the confocal volume. Additional information might be obtained from determining the rotational correlation time of the product molecules when performing measurements with linearly polarized light.[23] Due to the limited number of photons detectable, only excitation with circularly polarized light was possible in this experiment, and no information about interactions between the enzyme and product molecules can be obtained from these measurements (see the Supporting Information for a detailed discussion).

Nevertheless, the facts that only the intermediate succinyl-AlaAlaProPhe-Rh110 was detected in our measurement and that this intermediate does most likely not interact with the enzyme strongly allow us to draw direct conclusions about the enzymatic reaction itself. It contradicts the assumption of the tunneling effect[33,34] for this particular system. In the presence of tunneling, the intermediate of the two-step hydrolysis would undergo rotational motion and would immediately be cleaved by the enzyme to yield Rh110.[34] If this was the case, the formation of Rh110 would be detected with a high frequency. Only a small number of events with the lifetime of Rh110 was observed, however, that also varied between different experiments (see the Supporting Information).

The absence of tunneling is also supported by the catalytic mechanism of α-chymotrypsin that involves two steps: acylation of the enzyme active site resulting in a covalent enzyme−peptide complex, followed by deacylation and release of the peptide. The hydrolysis product containing the dye molecule is released first, while the peptide remains bound to the enzyme. It is, therefore, not likely that a strong interaction between the generated dye and the enzyme can take place. Also, no rebinding of the intermediate can occur as long as the peptide is still bound to the enzyme. The tunneling effect might be more likely if the dye part would dissociate from the enzyme after release of the peptide.

dx.doi.org/10.1021/jp310663v | J. Phys. Chem. B 2013, 117, 1252−1260

Once the produced intermediate is released from the enzyme, it will be free in solution and compete with the original substrate for binding to the active site. As a very high concentration of substrate was used in the experiment, many more substrate molecules were available for binding to the enzyme. Using the following assumptions, the number of intermediate molecules accumulating in solution during the measurement time can be calculated: (i) all enzymes present in the agarose solution remain on the surface during spin coating, (ii) all of these enzymes hydrolyze the substrate with a frequency of 42 turnovers/s, (iii) the binding affinity and the rate of bond cleavage are identical for each individual bond of both the substrate and the intermediate. Under these conditions, the number of intermediate molecules produced during the overall time of the measurement (1600 s) is roughly 10^{14}. The amount of substrate molecules, however, is approximately 10^{16} in a 30 μM solution. From this calculation, it becomes clear immediately that the chance for an intermediate molecule to bind to the enzyme and to be hydrolyzed to Rh110 is extremely small even after a measurement time of 1600 s (Figure S2, Supporting Information).

Having been able to identify this intermediate and to investigate the tunneling effect exemplifies the potential of single molecule experiments in the study of enzyme kinetics beyond the study of conformational dynamics. The tunneling effect has been a matter of debate for decades and can now be analyzed with our single molecule approach. Moreover, being able to measure only the hydrolysis of the original substrate into the intermediate at the single molecule level now for the first time provides the possibility of determining the kinetic parameters of the first step of the double-hydrolysis reaction. This is not possible in an ensemble measurement based on the fluorescence intensity. Detecting entirely the first step of the hydrolysis reaction further has two direct consequences for the usefulness of double-substituted Rh110-based protease substrates for single molecule experiments. Most importantly, a reaction scheme with 1:1 stoichiometry is obtained; i.e., every enzymatic turnover results in a detectable fluorescent product. This is an important prerequisite for the data analysis facilitating the construction of accurate kinetic schemes. On the other hand, the low brightness of the intermediate yields time traces with a low signal-to-noise ratio (approximately 2.5:1), complicating the assignment of the fluorescent on-states. This problem can only be overcome by designing new substrates with 1:1 stoichiometry that release a fluorophore with a higher brightness such as morpholinecarbonyl-rhodamine 110.[35]

To conclude, the multiparameter approach has additional advantages that have not been considered in this study. Multiparameter data can be utilized to identify on- and off-states that cannot be assigned to the main population (see the Supporting Information for examples). This allows for an additional cleanup step in the data analysis procedure. Further, if certain subpopulations can be identified as intermediates of the enzymatic reaction, they can be treated separately, providing additional details about the reaction mechanism. This might be especially relevant for FRET-based substrates where the high FRET species binds to the enzyme, gets cleaved, and dissociates. In a FRET reporter system, not only the intensity will be altered as a result of the enzymatic reaction but also the fluorescence lifetime. Multiparameter detection applied to enzymatic reactions, therefore, opens up a number of possibilities to investigate enzyme mechanisms and enzyme kinetics. It provides information about substeps of an enzymatic reaction cycle that is inaccessible with other single molecule detection schemes.

CONCLUSIONS

We have applied time-resolved fluorescence detection to study the enzymatic hydrolysis of a double-substituted fluorogenic substrate at the single molecule level. On the basis of the measured lifetimes, it was possible to differentiate the products of the first and second peptide cleavage. We have shown that at high substrate concentrations only the product of the first cleavage step is detected and that no intermediate tunneling takes place in the studied reaction. Comparing the fluorescence lifetimes of the off-states and the on-states, no differences are observed, indicating that the fluorescent reporter system itself is the main source of background photons. Further, no or only weak interactions between the produced dye molecule and the enzyme are taking place. Consequently, no improvement in the on−off assignment could be achieved using the time-resolved approach, although new mechanistic and kinetic information could be obtained. It can be expected that an improvement in the assignment of the on/off states will be possible for other reporter systems, such as FRET-labeled peptides. Having demonstrated its power to unveil the detailed nature of the two-step hydrolysis reaction catalyzed by a single α-chymotrypsin molecule, we expect that multiparameter detection will provide us with a generic and valuable single molecule approach to promote our understanding of enzymatic reactions.

ASSOCIATED CONTENT

Supporting Information

The data of two other enzymes, the data from the linear dichroism analysis, as well as the time evolution of the lifetimes for an individual enzyme. This material is available free of charge via the Internet at http://pubs.acs.org.

AUTHOR INFORMATION

Corresponding Author

*Address: Radboud University Nijmegen, Institute for Molecules and Materials, Department of Molecular Materials, Heyendaalseweg 135, 6525 AJ Nijmegen, The Netherlands (K.B.); Molecule & Life Nonlinear Sciences Laboratory, Research Institute for Electronic Science, Hokkaido University, Kita-20 Nishi-10, Kita-ku, Sapporo, Hokkaido 001-0020, Japan (C.-B.L.). Phone: +31 (0)24 365 2464 (K.B.); +81 (11) 706 9458 (C.-B.L.). Fax: +31 (0)24 365 2929 (K.B.); +81 (11) 706 9458 (C.-B.L.). E-mail: k.blank@science.ru.nl (K.B.); cbli@es.hokudai.ac.jp (C.-B.L.).

Notes

The authors declare no competing financial interest.

ACKNOWLEDGMENTS

Financial support of the “Fonds voor Wetenschappelijk Onderzoek FWO” (grants G.0402.09, G.0413.10, G.0697.11), the K. U. Leuven Research Fund (GOA 2011/03), the Flemish government (Long term structural funding − Methusalem funding CASAS METH/08/04), the Federal Science Policy of Belgium (IAP-VI/27), and the Hercules Foundation is gratefully acknowledged (T.G.T. and J.H.). K.B. acknowledges support from a long-term fellowship from the Human Frontier

Science Program (HFSP) and a VIDI grant from The Netherlands Organisation for Scientific Research (NWO). C.-B.L. and T.K. acknowledge support from JSPS, HFSP, Grant-in-Aid for Research on Priority Area 'Innovative nanoscience', MEXT.

REFERENCES

(1) Karplus, M.; Kuriyan, J. *Proc. Natl. Acad. Sci. U.S.A.* **2005**, *102*, 6679−6685.
(2) Henzler-Wildman, K.; Kern, D. *Nature* **2007**, *450*, 964−972.
(3) Swint-Kruse, L.; Fisher, H. F. *Trends Biochem. Sci.* **2008**, *33*, 104−112.
(4) Blank, K.; De Cremer, G.; Hofkens, J. *Biotechnol. J.* **2009**, *4*, 465−479.
(5) Claessen, V. I.; Engelkamp, H.; Christianen, P. C.; Maan, J. C.; Nolte, R. J.; Blank, K.; Rowan, A. E. *Annu. Rev. Anal. Chem.* **2010**, *3*, 319−340.
(6) Ha, T.; Ting, A. Y.; Liang, J.; Caldwell, W. B.; Deniz, A. A.; Chemla, D. S.; Schultz, P. G.; Weiss, S. *Proc. Natl. Acad. Sci. U.S.A.* **1999**, *96*, 893−898.
(7) Chen, Y.; Hu, D. H.; Vorpagel, E. R.; Lu, H. P. *J. Phys. Chem. B* **2003**, *107*, 7947−7956.
(8) Kuznetsova, S.; Zauner, G.; Aartsma, T. J.; Engelkamp, H.; Hatzakis, N.; Rowan, A. E.; Nolte, R. J.; Christianen, P. C.; Canters, G. W. *Proc. Natl. Acad. Sci. U.S.A.* **2008**, *105*, 3250−3255.
(9) Goldsmith, R. H.; Tabares, L. C.; Kostrz, D.; Dennison, C.; Aartsma, T. J.; Canters, G. W.; Moerner, W. E. *Proc. Natl. Acad. Sci. U.S.A.* **2011**, *108*, 17269−17274.
(10) Yang, H.; Luo, G.; Karnchanaphanurach, P.; Louie, T. M.; Rech, I.; Cova, S.; Xun, L.; Xie, X. S. *Science* **2003**, *302*, 262−266.
(11) Zhang, Z.; Rajagopalan, P. T.; Selzer, T.; Benkovic, S. J.; Hammes, G. G. *Proc. Natl. Acad. Sci. U.S.A.* **2004**, *101*, 2764−2769.
(12) van Oijen, A. M.; Blainey, P. C.; Crampton, D. J.; Richardson, C. C.; Ellenberger, T.; Xie, X. S. *Science* **2003**, *301*, 1235−1238.
(13) Werner, J. H.; Cai, H.; Jett, J. H.; Reha-Krantz, L.; Keller, R. A.; Goodwin, P. M. *J. Biotechnol.* **2003**, *102*, 1−14.
(14) Harris, T. D.; Buzby, P. R.; Babcock, H.; Beer, E.; Bowers, J.; Braslavsky, I.; Causey, M.; Colonell, J.; Dimeo, J.; Efcavitch, J. W.; et al. *Science* **2008**, *320*, 106−109.
(15) Xu, M.; Fujita, D.; Hanagata, N. *Small* **2009**, *5*, 2638−2649.
(16) Yildiz, A.; Forkey, J. N.; McKinney, S. A.; Ha, T.; Goldman, Y. E.; Selvin, P. R. *Science* **2003**, *300*, 2061−2065.
(17) Rocha, S.; Hutchison, J. A.; Peneva, K.; Herrmann, A.; Müllen, K.; Skjot, M.; Jorgensen, C. I.; Svendsen, A.; De Schryver, F. C.; Hofkens, J.; et al. *ChemPhysChem* **2009**, *10*, 151−161.
(18) Lu, H. P.; Xun, L.; Xie, X. S. *Science* **1998**, *282*, 1877−1882.
(19) Velonia, K.; Flomenbom, O.; Loos, D.; Masuo, S.; Cotlet, M.; Engelborghs, Y.; Hofkens, J.; Rowan, A. E.; Klafter, J.; Nolte, R. J.; et al. *Angew. Chem., Int. Ed.* **2005**, *44*, 560−564.
(20) English, B. P.; Min, W.; van Oijen, A. M.; Lee, K. T.; Luo, G.; Sun, H.; Cherayil, B. J.; Kou, S. C.; Xie, X. S. *Nat. Chem. Biol.* **2006**, *2*, 87−94.
(21) De Cremer, G.; Roeffaers, M. B.; Baruah, M.; Sliwa, M.; Sels, B. F.; Hofkens, J.; De Vos, D. E. *J. Am. Chem. Soc.* **2007**, *129*, 15458−15459.
(22) Martinez, V. M.; De Cremer, G.; Roeffaers, M. B.; Sliwa, M.; Baruah, M.; De Vos, D. E.; Hofkens, J.; Sels, B. F. *J. Am. Chem. Soc.* **2008**, *130*, 13192−13193.
(23) Schaffer, J.; Volkmer, A.; Eggeling, C.; Subramaniam, V.; Striker, G.; Seidel, C. A. M. *J. Phys. Chem. A* **1999**, *103*, 331−336.
(24) Rothwell, P. J.; Berger, S.; Kensch, O.; Felekyan, S.; Antonik, M.; Wohrl, B. M.; Restle, T.; Goody, R. S.; Seidel, C. A. *Proc. Natl. Acad. Sci. U.S.A.* **2003**, *100*, 1655−1660.
(25) Widengren, J.; Kudryavtsev, V.; Antonik, M.; Berger, S.; Gerken, M.; Seidel, C. A. *Anal. Chem.* **2006**, *78*, 2039−2050.
(26) Terentyeva, T. G.; Engelkamp, H.; Rowan, A. E.; Komatsuzaki, T.; Hofkens, J.; Li, C. B.; Blank, K. *ACS Nano* **2012**, *6*, 346−354.
(27) Enderlein, J.; Goodwin, P. M.; Van Orden, A.; Ambrose, W. P.; Erdmann, R.; Keller, R. A. *Chem. Phys. Lett.* **1997**, *270*, 464−470.
(28) Herten, D. P.; Tinnefeld, P.; Sauer, M. *Appl. Phys. B: Lasers Opt.* **2000**, *71*, 765−771.
(29) Brismar, H.; Trepte, O.; Ulfhake, B. *J. Histochem. Cytochem.* **1995**, *43*, 699−707.
(30) Suhling, K.; Siegel, J.; Phillips, D.; French, P. M.; Leveque-Fort, S.; Webb, S. E.; Davis, D. M. *Biophys. J.* **2002**, *83*, 3589−3595.
(31) Melhado, L. L.; Peltz, S. W.; Leytus, S. P.; Mangel, W. F. *J. Am. Chem. Soc.* **1982**, 104.
(32) Leytus, S. P.; Melhado, L. L.; Mangel, W. F. *Biochem. J.* **1983**, *209*, 299−307.
(33) Hofmann, J.; Sernetz, M. *Anal. Biochem.* **1983**, *131*, 180−186.
(34) Huang, Z. J. *Biochemistry* **1991**, *30*, 8535−8540.
(35) Terentyeva, T. G.; Van Rossom, W.; Van der Auweraer, M.; Blank, K.; Hofkens, J. *Bioconjugate Chem.* **2011**, *22*, 1932−1938.
(36) Cotlet, M.; Hofkens, J.; Habuchi, S.; Dirix, G.; Van Guyse, M.; Michiels, J.; Vanderleyden, J.; De Schryver, F. C. *Proc. Natl. Acad. Sci. U.S.A.* **2001**, *98*, 14398−14403.
(37) Watkins, L. P.; Yang, H. *J. Phys. Chem. B* **2005**, *109*, 617−628.
(38) Zhang, K.; Chang, H.; Fu, A.; Alivisatos, A. P.; Yang, H. *Nano Lett.* **2006**, *6*, 843−847.
(39) Cramer, H. *Mathematical Methods of Statistics*; Princeton University Press: Princeton, NJ, 1946.
(40) Rao, C. R. *Proc. Cambridge Philos. Soc.* **1949**, *45*, 213−218.
(41) Maus, M.; Cotlet, M.; Hofkens, J.; Gensch, T.; De Schryver, F. C.; Schaffer, J.; Seidel, C. A. *Anal. Chem.* **2001**, *73*, 2078−2086.
(42) Apanasovich, V. V.; Novikov, E. G. *Opt. Commun.* **1990**, *78*, 279−282.
(43) Boens, N.; Qin, W.; Basaric, N.; Hofkens, J.; Ameloot, M.; Pouget, J.; Lefevre, J. P.; Valeur, B.; Gratton, E.; vandeVen, M.; et al. *Anal. Chem.* **2007**, *79*, 2137−2149.
(44) Baba, A.; Komatsuzaki, T. *Proc. Natl. Acad. Sci. U.S.A.* **2007**, *104*, 19297−19302.
(45) Li, C. B.; Yang, H.; Komatsuzaki, T. *Proc. Natl. Acad. Sci. U.S.A.* **2008**, *105*, 536−541.
(46) Li, C. B.; Yang, H.; Komatsuzaki, T. *J. Phys. Chem. B* **2009**, *113*, 14732−14741.
(47) Schuetz, P.; Wuttke, R.; Schuler, B.; Caflisch, A. *J. Phys. Chem. B* **2010**, *114*, 15227−15235.
(48) Schroeyers, W.; Vallee, R.; Patra, D.; Hofkens, J.; Habuchi, S.; Vosch, T.; Cotlet, M.; Müllen, K.; Enderlein, J.; De Schryver, F. C. *J. Am. Chem. Soc.* **2004**, *126*, 14310−14311.